Carbohydrate Polymers 86 (2011) 1525–1532

Contents lists available at ScienceDirect

Carbohydrate Polymers

journal homepage: www.elsevier.com/locate/carbpol

Kinetics of starch hydrolysis and glucose mutarotation studied by NMR chemical exchange saturation transfer (CEST)

Anthony C. Dona[a,b], Guilhem Pages[a], Philip W. Kuchel[a,*]

[a] School of Molecular Bioscience, University of Sydney, NSW 2006, Australia
[b] Centre for Nutrition and Food Sciences, Hartley Teakle Building 83, The University of Queensland, Brisbane, QLD 4072, Australia

ARTICLE INFO

Article history:
Received 31 March 2011
Accepted 18 June 2011
Available online 5 July 2011

Keywords:
Chemical exchange saturation transfer (CEST)
Digestion kinetics
Mutarotation
Time-resolved nuclear magnetic resonance spectroscopy
NMR
z-Spectrum

ABSTRACT

The –OH resonance on $-C_1$ of the α and β-anomers of glucose that are normally invisible in ^{1}H NMR spectra, was used to monitor the reaction kinetics of starch hydrolysis in aqueous solutions. The exchangeable protons on glucose were detected indirectly through their exchange with water protons, and hence the water resonance, by using selective radiofrequency (RF) saturation at the absorption frequency of the hydroxyl protons. The saturated population of –OH spins exchanged rapidly with the water proton population, leading to the partial suppression of the water signal. Mutarotation of the anomers of glucose and starch digestion kinetics measured this way were consistent with those readily obtained by other more direct, but less sensitive, NMR methods. The chemical exchange saturation transfer (CEST) technique is useful in favourable circumstances when signals from non-exchangeable protons are not resolved in a crowded region of the spectrum. Thus the ^1H_2O signal is so relatively large that its dynamic range is high and it gives greatly enhanced sensitivity for (indirectly) detecting much less abundant saccharide species.

1. Introduction

The kinetics of enzyme-catalyzed starch digestion is a vigorously researched area, however current methods used to study them *in vivo* are costly; and the relevance to diet-management of analytical data on glucose release from foods is controversial and therefore in need of new analytical approaches (DeVries, 2007). The present work was directed at developing an *in vitro* method of analysis to predict *in vivo* digestion of carbohydrates in complex mixtures such as food. The protons on the –OH groups of starch chains and glucose molecules are in relatively rapid exchange with H_2O protons in aqueous solution; this finding can be exploited to study the enzyme kinetics of reactions involving saccharides by using saturation transfer experiments to monitor the emergence of free glucose. Thus, our aim here was to develop NMR-based analysis that exploits this exchange, and to apply it to the characterization of the kinetics of starch digestion.

NMR spectroscopy has been used to measure the rates of chemical exchange reactions for more than four decades (Forsen & Hoffman, 1963; Kim, Gillen, Landman Bennett, Zhou, & van Zijl Peter, 2009; Kuchel, Bulliman, Chapman, & Kirk, 1987; Zhou & van Zijl, 2006; Zhou, Wilson, Sun, Klaus, & van Zijl, 2004). The analysis of the special spectra that were generated required the NMR Bloch equations to be modified to include terms that describe the chemically mediated exchange of magnetization. Thus proton transfer rates between ammonium ions and solvent water molecules were able to be measured (McConnell & Thompson, 1959). Another early example of chemical exchange saturation transfer (CEST) analysis was the measurement of the rate of proton transfer between salicylaldehyde and water (Forsen & Hoffman, 1963). Recently CEST techniques have generated much interest as a means of producing contrast in magnetic resonance images (Guivel-Scharen, Sinnwell, Wolff, & Balaban, 1998; Zhang, Merritt, Woessner, Lenkinski, & Sherry, 2003); and yet, for many years saturation transfer and more general magnetization transfer methods have enjoyed wide biochemical applications in determining rate constants for enzyme-catalyzed and membrane transport reactions (Brindle, Brown, Campbell, Grathwohl, & Kuchel, 1979; Kuchel et al., 1987; Labotka, Lundberg, & Kuchel, 1995; Szekely, Chapman, Bubb, & Kuchel, 2006).

For spin-1/2 nuclei like ^{1}H, the Boltzmann equation explains the unequal distribution of populations of nuclear-spin eigenstates, aligned either with or against the main magnetic field of the NMR spectrometer ($\mathbf{B}_0$). Magnetic saturation by selective radiofrequency (RF) irradiation at the resonance frequency of a nuclear population equalises the populations of the two eigenstates. If a population

Abbreviations: CEST, chemical exchange saturation transfer; CPMG, Carr, Purcell, Meiboom, and Gill; GI, glycemic index; MTRasym, magnetization-transfer asymemetry ratio; NMR, nuclear magnetic resonance; PTE, proton transfer enhancement; RF, radiofrequency.

* Corresponding author. Tel.: +65 6478 8743.
E-mail address: philip_kuchel@sbic.a-star.edu.sg (P.W. Kuchel).

0144-8617/$ – see front matter © 2011 Elsevier Ltd. All rights reserved.
doi:10.1016/j.carbpol.2011.06.056

is in chemical exchange with another population this saturation will be, at least partially, passed to it. For the purpose of this study we consider a system where exchangeable protons of –OH groups on a particular type of molecule (Pool A) are in exchange with the protons of the solvent water (Pool B) (Scheme 1),

$$\text{G-O}\underline{\text{H}}_{\text{A}} + \text{HO}\underline{\text{H}}_{\text{B}} \underset{k_{-1}}{\overset{k_1}{\rightleftharpoons}} \text{G-O}\underline{\text{H}}_{\text{B}} + \text{HO}\underline{\text{H}}_{\text{A}} \quad (1)$$

where k_1 is the forward and k_{-1} is the reverse-rate constant characterizing the reaction. Saturating the magnetization of the solute population causes no solute resonance to be observed in the spectrum that is generated after applying a $\pi/2$ sampling pulse to give a free induction decay (FID). As the nuclei in the molecules of Pool A are in chemical exchange with those in Pool B saturation of magnetization is transferred from Pool A to Pool B. The net result is a concomitant decrease in the NMR signal intensity from the nuclei in Pool B.

A notable feature of this experiment is that the solute molecules do not need to be highly concentrated, or even able to be detected in the NMR spectrum, for their nuclear magnetization to be saturated and for the saturation transfer from them to dramatically affect the signal from the much larger solvent population. In other words, when the saturating RF field is applied at the resonance frequency of the solute molecules, the solvent signal (which is evidently very large in comparison to that of the solute in the present cases) is suppressed by proton exchange to an extent where the change in magnetization (ΔM; viewed as a negative signal) is much larger than the direct signal from the solute. Thus the signal-to-noise ratio for detecting the solute is greatly enhanced.

The water resonance intensity that remains when saturating with frequency-selective RF irradiation at different offsets from the centre of the water resonance can be graphed to yield a so-called *z*-spectrum. Although an increase in the rate of exchange of –OH protons reduces their direct visibility in ^{1}H NMR spectra, the sensitivity to detection is enhanced by recording a *z*-spectrum because of the proton exchange with the relatively massive H_2O population with its large NMR signal. The rate of proton exchange is such that the CEST effect can be used with the –OH groups of glucose, and glucose residues, at concentrations in solution where the corresponding directly recorded ^{1}H NMR spectral peaks are barely visible.

Only at temperatures close to 0 °C do the high resolution ^{1}H NMR spectra of carbohydrate polymers like glycogen and starch, have well-defined resonances assigned to protons on –OH groups. The line-width of these resonances gradually broaden as the temperature is increased, causing them to eventually disappear at 'biological' temperatures (van Zijl, Jones, Ren, Malloy, & Sherry, 2007). However, CEST is valuable for analysing biological reactions involving –OH groups that are normally NMR-invisible at biological temperatures since they can still be detected, albeit indirectly.

In carbohydrate samples the CEST effect is more pronounced with higher concentrations, as well as having significant dependence on temperature and type of buffer; the proton exchange is acid–base catalyzed so other proton-exchanging groups in solution affect the lifetime of the protonated –OH. It is often difficult to quantify accurately the variations in signal intensity brought about by RF irradiation of one spin population if the spectral resonances of the two exchanging populations are not well resolved; there can be a significant 'spill over' effect, suppressing the second resonance due to the non-selectivity of the saturating RF field. To control for this potential experimental artifact the magnitude of the CEST effect is described in terms of a magnetization-transfer asymmetry ratio (MTR_{asym}), a parameter that is defined as

$$\text{MTR}_{\text{asym}}(\Delta\omega) = \frac{S(-\Delta\omega) - S(\Delta\omega)}{S_0} \quad (2)$$

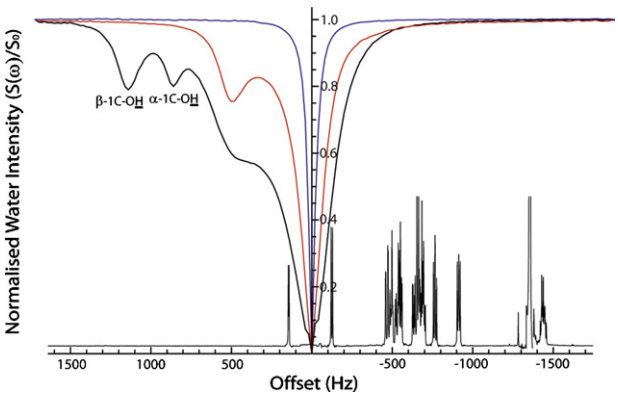

Fig. 1. ^{1}H NMR *z*-spectra of glucose and starch in water and acetate buffer: solvent only (*blue*); 100 mmol L^{-1} (glucose equivalent) autoclaved rice starch (*red*); and 100 mmol L^{-1} glucose (*black*) in 2 mmol L^{-1} acetate buffer at 37 °C. In the figure the water frequency was arbitrarily set to 0 Hz. *Overlay:* ^{1}H NMR spectrum of 100 mmol L^{-1} glucose in acetate buffer at 37 °C. (For interpretation of the references to color in this figure legend, the reader is referred to the web version of the article.)

where $\Delta\omega$ is the difference between the irradiation frequency and the centre of water resonance, $-\Delta\omega$ is the offset in the opposite direction of the centre of the water resonance, $S(\Delta\omega)$ and $S(-\Delta\omega)$ are the water intensities after a long pre-saturation pulse at the offset frequency and the offset on the opposite side of the water signal, respectively. S_0 is the water resonance intensity at a very large irradiation offset at which the water-resonance intensity is unaffected by the field. The parameter MTR_{asym} is most useful if it can be shown that the envelope of the saturating RF field is symmetrical. This was confirmed experimentally, in the present work, by measuring the *z*-spectrum of only the solvent used for monitoring reactions by CEST (Fig. 1).

Measuring the intensity of the perturbed water signal significantly enhances the signal-to-noise ratio obtained when compared to monitoring exchangeable protons directly (Goffeney, Bulte, Duyn, Bryant, & van Zijl, 2001). For fast exchange between two spin populations, each giving a resolved single signal, it can be shown that the proton transfer enhancement (PTE) is (Eq. (3)),

$$\text{PTE} = \frac{\alpha k' M_{\text{W}} N}{(1-x)R_{1\text{wat}} + xk}\left(1 - e^{-[(1-x)R_{1\text{wat}} + xk]t_{\text{sat}}}\right) \quad (3)$$

where α is the saturation efficiency ($0 < \alpha < 1$), k' the pseudo-first-order forward rate constant of chemical exchange (Eq. (4)), M_{w} the molecular weight, N is the number of exchangeable protons of a particular type per molecular weight unit, and x the fractional concentration of exchangeable protons. The exponential term accounts for the influence of back-exchange and the longitudinal relaxation rate constant ($R_{1\text{wat}} = 1/T_{1\text{wat}}$) of water protons on the build-up of this effect during the saturation period (t_{sat}). The pseudo-first-order rate constant (k') of exchange depends on the concentration of glucose (Eq. (4)), so the PTE depends on glucose concentration which is discussed later.

$$k' = k[G] \quad (4)$$

where k is the rate constant of proton exchange between glucose and water, and $[G]$ is the concentration of glucose.

Controversy surrounds the *in vivo* measure of the glycemic index (GI), including its reproducibility and therefore its relevance to nutrition (Barclay et al., 2008; DeVries, 2007; Livesey, Taylor, Hulshof, & Howlett, 2008). Conducting experiments on commercial foods to estimate their GI, or other *in vivo* measures, is costly; so recent research has been aimed at developing *in vitro* methods to predict GI or some equivalent 'metric' that can be used in nutritional analysis (Garsetti et al., 2005; Goni, Garcia-Alonso, & Saura-Calixto, 1997; Okuda, Aramaki, Koseki, Satoh, & Hashizume, 2005).

The rate of sugar release from enzymic starch digestion is of biological importance as it affects many areas of human health (Brand-Miller, Holt, Pawlak, & McMillan, 2002; Thornley, McRobbie, Eyles, Walker, & Simmons, 2008; Wolever et al., 2008). The rate of sugar release depends on two main factors. The first is the molecular architecture and physicochemical characteristics of the starch granule, at all its "six levels of structure" (Ao et al., 2007; French & Knapp, 1950; Kerr, Cleveland, & Katzbeck, 1951; Kruger & Marchylo, 1985). Research correlating the botanical origin, largely responsible for the architecture of the starch granule, with both *in vivo* and *in vitro* digestibility is advanced; this is a correlation and does not follow the causal relationship of starch granule biosynthesis (biosynthesis causes structural properties that determine digestibility) (Goni et al., 1997; Jenkins et al., 2002; Thompson, 2000). The second feature affecting the rate of sugar release is the hydration or physical conformations that starch granules assume in aqueous solution; these conformations control digestibility. Both heat and pressure during the preparation of starch suspensions alter the progression towards gelatinisation, which increases the availability of polysaccharide starch chains to digestive enzymes, thus affecting the rate of glucose release (Chung, Lim, & Lim, 2006; Chung, Yoo, & Lim, 2005).

2. Experimental

2.1. Materials

Anhydrous α-D-glucose (AF404308; Ajax Finechem, NSW, Australia) was used for calibrating concentrations from ^{1}H NMR spectra in starch digestion experiments. For studies relating to starch digestion, glucoamylase (E.C. 3.2.1.3) from *Aspergillus niger* (A7095, Sigma, St Louis, MO) was obtained at a concentration of 300 U mL^{-1}, where a single unit of enzyme is defined as that amount which hydrolyzes the α (1,4) linkage of maltose at a rate of 1 μmol min^{-1} at 25 °C. The enzyme was added to rice starch (S-7260, Sigma, St Louis, MO) during digestion analysis.

The buffer solution mainly used was 2 mmol L^{-1} acetate (sodium acetate, D3247; and glacial acetic acid, AH312068; Ajax Finechem) at pH 5.3 in H_2O. Potassium hydrogen phthalate (399, Ajax Finechem) was also used for some experiments as indicated in the text.

2.2. Methods

2.2.1. ^{1}H nuclear magnetic resonance

All NMR spectra were acquired on a Bruker Avance III spectrometer (Karlsruhe, Germany), equipped with a 9.4 T wide-bore vertical magnet (Oxford Instruments, Oxford, UK), operating at an RF of 400.09 MHz for ^{1}H detection, using a triple resonance inverse (TXI) probe. The probe temperature was set to 37 °C for all experiments. The 90° pulse duration was ~11.5 μs; and the acquisition time (aq) and relaxation delay (d_1) were 8 s and 2 s, respectively. The pre-saturation pulse had a duration of 10 s and a B_1 of 1.9 μT. Each spectrum was derived from two transients. Chemical shifts were calibrated using the resonance from H_2O at 0.000 Hz. Exponential line broadening of 1 Hz was used with no zero-filling prior to Fourier transformation of the FID. The data were recorded and processed using TOPSPIN 2.1 software (Bruker).

To calibrate the ^{1}H NMR intensities of the –C_1O<u>H</u> resonances of α- and β-reducing ends of glucose, z-spectra of 10 D-glucose standards were recorded at concentrations ranging from 10 to 100 mM. To quantify the concentration of glucose produced during starch digestion experiments, standard solutions made up of mixtures of autoclaved starch and free glucose were diluted to each contain a total of 100 mM glucose units (i.e., 10 mM of glucose and 90 mM glucose equivalent starch and so forth). Nine standards were constructed with free glucose concentrations ranging between 0 and 100 mM. For each standard, a set of 181 spectra were recorded, with the pre-saturation RF pulse shifted in frequency by 20 Hz. The integral of the water resonance was plotted against the saturation frequency to create each z-spectrum.

All digestion reactions were carried out in 2 mmol L^{-1} sodium acetate buffer, at pH 5.3 made up in H_2O. Prior to enzyme addition, a spectrum of each sample was acquired, and the corresponding asymmetry at the –C_1O<u>H</u> resonance of the α- and β-reducing ends was recorded. Subsequently, glucoamylase enzyme solution (1.2 U mL^{-1}) was added to the starch solution samples and the asymmetry was measured at the frequencies of interest over time. The delay between beginning the enzymic reaction and recording a ^{1}H NMR spectrum was precisely timed (~2 min); then up to 500 ^{1}H NMR spectra (~2 min each) were acquired sequentially to monitor the time course. To compare the method with other well developed NMR methods for monitoring the digestion of starch, a Carr, Purcell, Meiboom, and Gill (CPMG) pulse sequence was used, as described by Dona, Pages, Gilbert, Gaborieau, and Kuchel (2009).

2.2.2. Preparation of samples

Autoclaving is the most widely used technique for homogenising of starch suspensions, although many starch varieties do not solvate to homogeneity (Mukerjea, Slocum, Mukerjea, & Robyt, 2006). CEST experiments require samples to be solvated, and ideally homogeneous; however as with many NMR techniques spectra can be recorded from inhomogeneous samples (e.g., Dona et al., 2007, 2009; Mulquiney, Bubb, & Kuchel, 1999). Therefore, samples used for z-spectrum experiments were autoclaved at 121 °C for 30 min in a glass vial and then aliquots were transferred at room temperature to NMR tubes.

2.2.3. ^{1}H NMR spectral features of carbohydrates

The features in z-spectra of carbohydrates change significantly with carbohydrate type, concentration, buffer conditions and temperature (van Zijl et al., 2007). Saturation envelope experiments of acetate buffer alone displayed no asymmetric features on the H_2O resonance (Fig. 1). Upon running the same experiment on an autoclaved starch sample, in acetate buffer, a single asymmetric feature appeared due to the four –O<u>H</u> groups that exist on glucose residues in starch chains. Saturation envelope analysis of glucose in acetate buffer revealed that its z-spectrum contained two additional characteristic features compared with autoclaved starch (Fig. 1). These features correspond to the exchange with H_2O from reducing end α- and β-G–O<u>H</u> signals (860 and 1140 Hz from the water peak, respectively). These offsets did not generate a significant asymmetrical feature in the z-spectrum from either buffer solution, or autoclaved starch samples (Fig. 2).

The MTR_{asym} (Eq. (2)) further clarifies the features observed in the z-spectra of measured samples (Fig. 1). The peaks present due to the –O<u>H</u> groups on the reducing end of glucose are better resolved than the other –O<u>H</u>s of glucose such that variations between samples can be more accurately quantified. The other –O<u>H</u> resonances in both glucose and starch molecules (C2, 3, 5 and 6) produce a single unresolved feature that is most prominent at 540 Hz (Fig. 2). The feature is more prominent in glucose than in autoclaved starch at comparable glucose unit concentrations, most likely due to a change in the exchange rate of equivalent protons in the two different sample. A small change in environment can significantly affect the proton exchange rate (van Zijl et al., 2007).

2.2.4. Influence of buffer type and concentration

Various buffer concentrations and types were explored to maximize the asymmetric signal from z-spectra of carbohydrates. To minimize the error encountered when monitoring the kinetics of

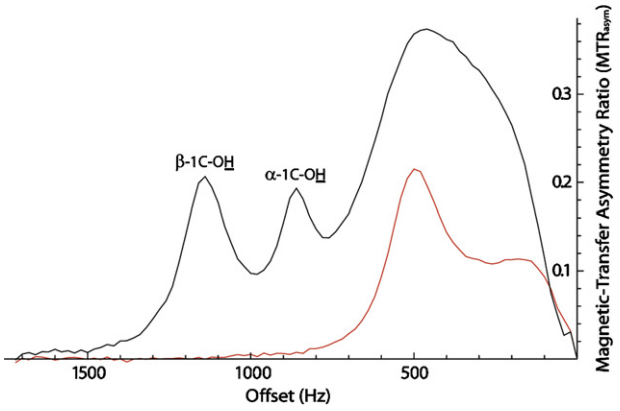

Fig. 2. Magnetization transfer asymmetry ratio of glucose and starch: 100 mmol L^{-1} glucose (*black*); and 100 mmol L^{-1} (glucose equivalent) rice starch (*red*) in 2 mmol L^{-1} acetate buffer at 37 °C. (For interpretation of the references to color in this figure legend, the reader is referred to the web version of the article.)

various carbohydrate reactions, the measured asymmetric signal needed to be maximised. Saturation envelope experiments were carried out on glucose in two buffer types, acetate and phthalate (pH 5.3), over a range of concentrations. A pH of 5.3 was chosen for many reasons including the glucoamylase used later for digestibility studies has optimal activity at this pH. Furthermore, initial studies showed the CEST experiments were found to give more resolved signals at pH 5.3 in acetate buffer.

The asymmetric features in both buffers increased in magnitude at lower buffer concentrations; at a given concentration, phthalate buffer gave a significantly more asymmetric signal than acetate buffer (Fig. 3). However, the signals measured in the *z*-spectrum of glucose in phthalate buffer were broader and less well-reolved than the signals recorded in acetate buffer. This poorer resolution in phthalate buffer is most prominently seen on the shoulder at 540 Hz, and it clearly had more definition in the sample recorded in acetate buffer (Fig. 3). The decrease in broadness of signals in acetate buffer was also clearly recognisable in the signal around 0 Hz due to water.

Acetate buffer was used rather than phthalate buffer for further studies as the *z*-spectrum of glucose had better definition, allowing the features to be more accurately monitored over time; acetate buffer was also chosen for consistency with digestibility studies carried out in previous research. The concentration of acetate buffer (2 mmol L^{-1}) chosen for kinetic analysis was relatively small in order to maximise the MTR_{asym}, however it was sufficiently large to hold the pH stable at 5.3 after starch or glucose addition.

Table 1
Comparison of the theoretically calculated and experimentally measured MTR_{asym} for each anomer of glucose.

Glucose anomer	Theoretical MTR_{asym}	Experimental MTR_{asym}
α	0.214 ± 0.003[a]	0.165 ± 0.008
β	0.222 ± 0.004	0.172 ± 0.010

[a] Denotes ± standard deviation.

3. Results and discussion

3.1. Theoretical magnetic transfer ratio asymmetry

As mentioned previously, monitoring of –OH protons indirectly through the perturbed water signal leads to a significant improvement in the signal-to-noise ratio compared with directly monitoring –OH signals. Theoretically the observed ratio of the water signal intensity, with ($S(\Delta\omega)$) and without (S_0) saturation of the exchangeable protons on the carbohydrate can be calculated (Eq. (5)):

$$\left(1 - \frac{S(\Delta\omega)}{S_0}\right) = \frac{[\text{carbohydrate}]\text{PTE}}{2[H_2O]} \quad (5)$$

where PTE is the theoretical proton transfer enhancement (Eq. (3)). Having calculated the $S(\Delta\omega)/S_0$ ratio, it is inherent from Eq. (2) that the MTR_{asym} observed for the features in a carbohydrate *z*-spectrum can be calculated theoretically (Table 1).

The normalised intensity of the water signal can be simulated over a range of glucose concentrations for different values of the first-order-rate constant (k_1) for proton exchange. The simulation to showed that as the glucose concentration increased the expected normalised intensity of the water signal decayed away rapidly. At a given concentration of glucose the theoretical normalised intensity of the water signal also decreased as the rate of exchange increased (Fig. 4).

To calculate the theoretical MTR_{asym}, ideal saturation efficiency ($\alpha = 1$) was assumed, and previously recorded data (Cho et al., 1991) were extrapolated to estimate the spin-lattice relaxation time of water in glucose solutions ($T_1 = 3.0 \pm 0.1$ s). The kinetic exchange rates were also estimated between the hydroxyl protons of glucose with water by extrapolation from recorded data (Fabri et al., 2005) for each anomer of glucose ($k_{1\alpha} = 2150\ s^{-1}$ and $k_{1\beta} = 700\ s^{-1}$). Using the respective concentrations of each anomer ($[G_\alpha] = 34$ mmol L^{-1}

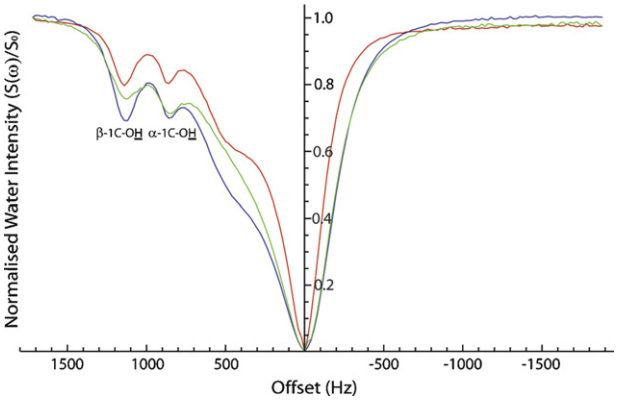

Fig. 3. The *z*-spectra of 100 mmol L^{-1} glucose in 2 mmol L^{-1} acetate buffer (*red*), 2 mmol L^{-1} phthalate buffer (*blue*), and 10 mmol L^{-1} phthalate buffer (*green*) with pH 5.3 at 37 °C. (For interpretation of the references to color in this figure legend, the reader is referred to the web version of the article.)

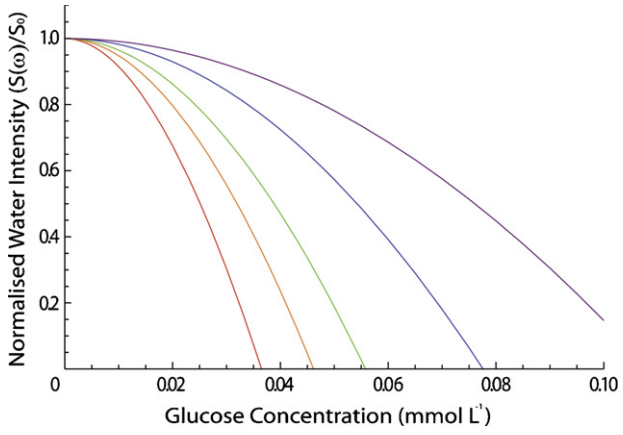

Fig. 4. Simulated normalized intensity of the water signal in glucose solutions at different first order rate constants for proton exchange (s^{-1}, 10000 (*red*), 6000 (*orange*), 4000 (*green*), 2000 (*blue*), 1000 (*purple*)). (For interpretation of the references to color in this figure legend, the reader is referred to the web version of the article.)

and $[G_\beta] = 64\,\text{mmol L}^{-1}$) the theoretical MTR_{asym} was calculated in 100 mmol L^{-1} glucose using Eqs. (2), (3) and (5).

Comparing the theoretical values with experimentally obtained measurements of the MTR_{asym} showed a close relationship. However, a significant difference existed between the values of MTR_{asym} measured experimentally and estimated theoretically (Table 1). The overestimation of theoretically calculated values for MTR_{asym} may be caused by fast rates of proton exchange not allowing full saturation before exchange, thereby reducing the saturation efficiency which was assumed to be 100% effective (i.e. $\alpha = 1$).

The saturation efficiency is reduced due to 'back exchange' of water protons from the magnetically saturated population occurring with high concentrations of exchangeable protons on the –OHs of the carbohydrates. This inherently reduces the CEST effect (Woods et al., 2006). At high exchange rates the analytical expression for PTE (Eq. (3)), used to calculate the MTR_{asym} does not hold, even for low concentrations of glucose. Exact fits of the data can be obtained by numerically regressing the Bloch equations (McMahon et al., 2006) onto them, however this approach lay beyond the scope of the present work. Back exchange and intra-hydroxyl exchange were not considered during the present study as the effect was negligible.

Considering the high exchange rate, the reduced saturation efficiency, α, can be estimated using the pulse power and the exchange rate constant:

$$\alpha = \frac{(\gamma B_1)^2}{(\gamma B_1)^2 + k^2} \tag{6}$$

where γB_1 is the power of the applied pulse; α was calculated using the known (set by the experimenter) applied pulse power, and the theoretical kinetic exchange rate constant(s). For the α-anomer of glucose the reduced saturation efficiency was estimated to be 97.9% and for the β-anomer it was 98.5%. The saturation efficiency of less than 100% provided a theoretical basis for understanding the experimental estimate of MTR_{asym} (Table 1).

3.2. Mutarotation

The kinetics of mutarotation of glucose have been successfully investigated by polarimetry (Kendrew and Moelwyn-Hughes, 1940), ^{1}H NMR (Dona et al., 2009) and ^{13}C NMR (Kuchel et al., 1988). To demonstrate the applicability of CEST to monitor reaction kinetics, the mutarotational kinetic constants of glucose were measured. Prior to kinetic measurements, a set of glucose standards (between 10 and 100 mmol L^{-1}) were analysed and the resulting *z*-spectra used to correlate MTR_{asym} to anomer concentration. The *z*-spectra of standards of increasing glucose concentration displayed increasing signals resulting from the α- and β-anomers at 860 and 1140 Hz from the water frequency, respectively. Although glucose concentration and MTR_{asym} signal are not expected to have a strictly linear relationship, it was found to be linear over the glucose concentrations used in this work.

Time courses of mutarotation were monitored by running CEST experiments. Rather than saturating across all frequencies, required to create *z*-spectra, the saturation pulse was cycled between three frequencies for each anomer to monitor the change in MTR_{asym} (Fig. 5). The water intensity was measured after long pre-saturation pulses at the offset frequency of the anomer, at the offset frequency on the opposite side of the water frequency of the anomer, and at a very large offset at which the water-signal intensity was not affected (i.e., for the α-anomer, 860, −860 and 1800 Hz). The MTR_{asym} was later calibrated to yield the concentration of each anomer over time and the kinetic constants of

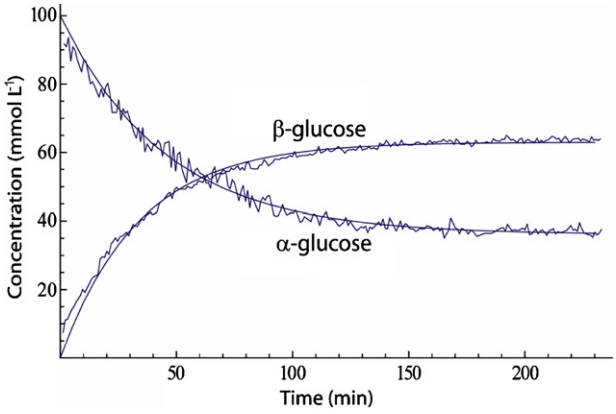

Fig. 5. Concentration of each anomer of glucose as estimated by CEST measurements during the mutarotation of α-D-glucose in 2 mmol L^{-1} acetate buffer at 25 °C. The asymmetry was measured at an offset of 1140 Hz (β-glucose) and 860 Hz (α-glucose) with calculated mutarotation parameters equal to $k_{M1} = (1.58 \pm 0.12) \times 10^{-4}\,\text{s}^{-1}$ and $k_{M-1} = (2.76 \pm 0.16) \times 10^{-4}\,\text{s}^{-1}$.

mutarotation were calculated by optimising the fit between Eqs. (7) and (8), and the data.

$$[\alpha(t)] = \frac{[A]_0(k_{M1}e^{-(k_{M1}+k_{M-1})t} + k_{M-1})}{k_{M1} + k_{M-1}} \tag{7}$$

$$[\beta(t)] = \frac{[A]_0(k_{M1} + k_{M-1}e^{-(k_{M1}+k_{M-1})t})}{k_{M1} + k_{M-1}} \tag{8}$$

where $[\alpha]$ is the concentration of the α-anomer, k_{M1} is the rate constant for conversion from α-glucoside to β-glucoside, k_{M-1} is that in the opposite direction, and $[A]_0$ is the original concentration of α-D-glucose.

3.3. Starch digestion by CEST

In order to monitor the kinetics of enzymic hydrolysis by CEST methodologies, first a set of intermediate standards were studied. Saturation envelope experiments were performed on a range of samples all containing the equivalent of 100 mmol L^{-1} glucose or glucose residues. The standards differed by the amount of glucose existing as a monomer or contained in starch molecules that had been solubilised by autoclaving. All three main features observed in the *z*-spectra (540, 860, 1140 Hz) increased in depth as the concentration of autoclaved starch was decreased and the concentration

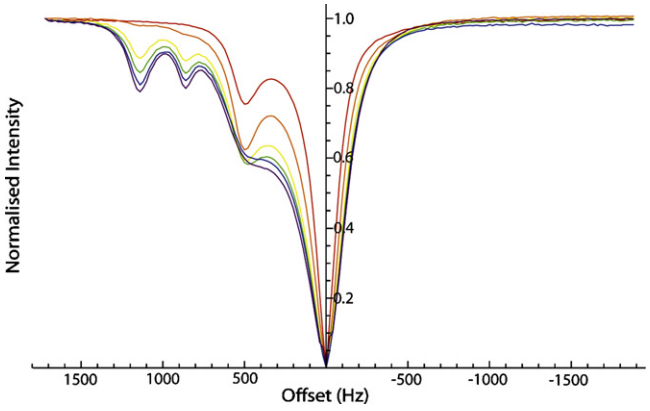

Fig. 6. ^{1}H NMR *z*-spectra from glucose and starch standards: glucose (mmol L^{-1}, 0 (*red*), 10 (*orange*), 40 (*yellow*), 60 (*green*), 90 (*blue*), 100 (*purple*)) with autoclaved starch in 2 mmol L^{-1} acetate buffer (pH 5.3). The standards were produced so the total glucose or glucose residue equivalent concentration (glucose plus autoclaved starch) was 100 mmol L^{-1}. (For interpretation of the references to color in this figure legend, the reader is referred to the web version of the article.)

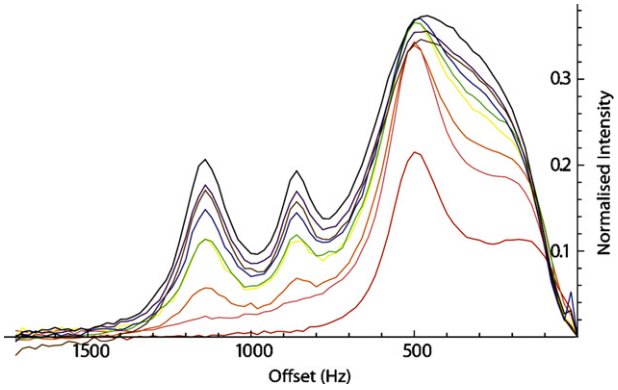

Fig. 7. Magnetization transfer asymmetry ratio, MTR_{asym}, for glucose and starch: glucose standards (mmol L^{-1}, 0 (*red*), 10 (*pink*), 20 (orange), 40 (*yellow*), 50 (*green*), 60 (*blue*), 80 (*purple*), 90 (*brown*), 100 (*black*)) of increasing concentration with autoclaved starch in 2 mmol L^{-1} acetate buffer (pH 5.3). The standards were compared so the total glucose or glucose residue concentration (glucose plus autoclaved starch) was 100 mmol L^{-1}. (For interpretation of the references to color in this figure legend, the reader is referred to the web version of the article.)

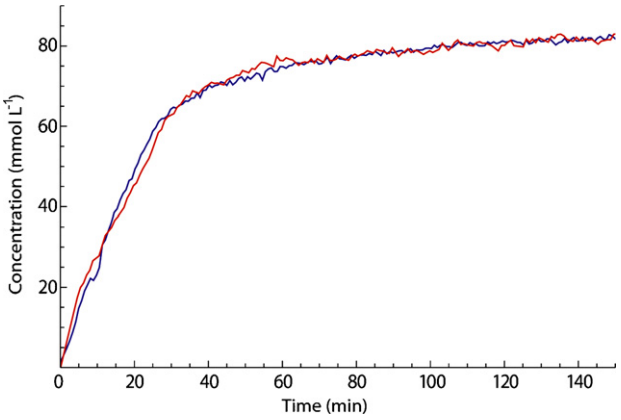

Fig. 9. Concentration of glucose produced when 100 mmol L^{-1} of autoclaved starch was digested by glucoamylase (1.2 U mL^{-1}) in 2 mmol L^{-1} acetate buffer (pH 5.3). Glucose concentration was measured by CPMG ^{1}H NMR experiments, with D_2O solvent (*blue*) and measured by CEST NMR in H_2O solvent (*red*). (For interpretation of the references to color in this figure legend, the reader is referred to the web version of the article.)

of glucose was increased (Fig. 6). This phenomenon allowed the hydrolysis of starch molecules by glucoamylase to be followed by the saturation transfer method.

To quantify the variation in the saturation features of standards, the effect was better described in terms of the MTR_{asym} parameter. The asymmetry displayed an increase in magnitude as the concentration of glucose was increased. The features of the α- and β-anomers displayed no clear change in shape although the minimum at 540 Hz broadened and became less well-defined as the concentration of glucose was increased. In 100 mmol L^{-1} (glucose equivalent) autoclaved starch the asymmetry of the minimum at 540 Hz was less intense than for standards with glucose present however it appeared to display more definition. The feature due to the four exchangeable protons of starch chains showed sufficient definition to enable it to be defined as two separate peaks (Fig. 7).

To normalise the measured asymmetry to the concentration of glucose in the sample a calibration curve between the measured MTR_{asym} and the concentration of each anomer was developed (Fig. 8). One would not expect the MTR_{asym} signal to be strictly linear with glucose concentration. As with any saturation phenomenon, the effect can only *approach* a maximum of 100%. The concentration at which maximum saturation is reached depends

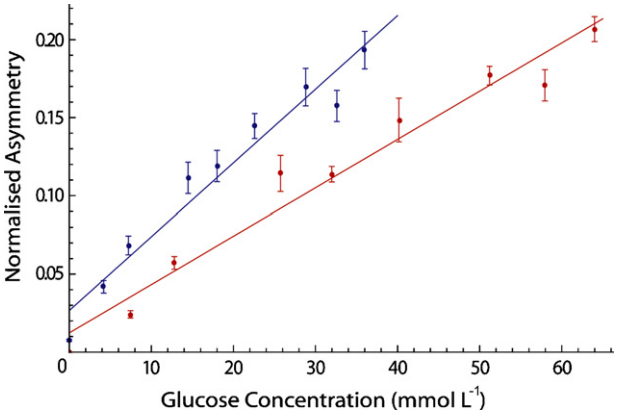

Fig. 8. Linear fits to the intensity of the MTR_{asym} at 860 and 1140 Hz corresponding to α-glucose (*blue*) and β-glucose (*red*) features in Fig. 7, respectively, against the concentration of each anomer. Best fit equations: α-anomer, NA = 0.00472[αG] + 0.02667; β-anomer, NA = 0.00309[βG] + 0.01235. (For interpretation of the references to color in this figure legend, the reader is referred to the web version of the article.)

on two parameters: (1) the concentration of exchangeable protons; and (2) the exchange rate constant(s). Maximum saturation is reached at lower concentrations when exchange rates are larger (Fig. 4). Linear dependence at concentrations below 50 mmol L^{-1} had been previously observed between the magnitudes of MTR_{asym} signals, as a function of glucose concentration; higher concentrations displayed non-linearity (van Zijl et al., 2007). However, a study of anomer concentrations up to 65 mmol L^{-1} in the present work was sufficiently close to linear to warrant calibrating glucose concentration with a straight line (Fig. 8). During the digestion of 100 mmol L^{-1} starch (glucose equivalent), the concentration of either anomer of glucose did not exceed 65 mmol L^{-1} such that the linear calibration was sufficient.

In a manner similar to the monitoring of the kinetics of mutarotation, the kinetics of digestion of starch was monitored by the CEST technique. Only the frequencies corresponding to the asymmetries of each anomer's minima were recorded, allowing for measurement of frequent time points. The concentration of glucose could then be calculated at any given time during the time course by using the standard calibration line (Fig. 8). Monitoring the enzymic digestions of autoclaved rice starch by CPMG methods displayed analogous kinetic results to those monitored by the saturation transfer method (Fig. 9). Therefore validation was provided to show that CEST is a practical method for monitoring the reaction kinetics of starch digestion, and mutarotation of glucose.

As with any methodology, there are specific advantages and disadvantages to the application of CEST compared with other reaction-monitoring techniques. Like any solution NMR technique, CEST requires the exchangeable proton groups of interest to be completely solvated in a relatively homogeneous solution. Further limitations to the application of CEST include the relatively high temperatures (≥25 °C) required to observe asymmetry in the *z*-spectrum due to the exchangeable protons. The features of the *z*-spectrum were very dependent on the environment in which they were monitored, and compared with classical CPMG ^{1}H NMR experiments the signals observed indirectly by CEST experiments were broader and less well-defined. Coincidently, the uncertainty of kinetic constants estimated in carbohydrate reactions using CEST techniques was larger than constants estimated using classical ^{1}H NMR CPMG experiments. However, the kinetic constants estimated by using either CPMG ^{1}H NMR or CEST experiments showed insignificant variation. The constants and their uncertainties estimated using the Michaelis–Menten equation for enzymic activity,

Table 2
Comparison of the estimates of the values of the Michaelis–Menten kinetic constants for digestibility obtained from the two NMR experimental techniques.

NMR technique	K_m (mmol L^{-1})	V_{max} (mmol L^{-1} s^{-1})
CPMG ^{1}H NMR	90 ± 3[a]	0.083 ± 0.008
CEST	83 ± 15	0.075 ± 0.015

[a] Denotes ± standard deviation.

as measured by the two experimental techniques, are given in Table 2.

As the application of CEST detects protons indirectly through the water signal it provides certain advantages over classical NMR techniques; for instance exchangeable protons undetectable by conventional NMR techniques become detectable. Recently, the CEST approach has been applied to monitor the breakdown of glycogen in mouse liver (van Zijl et al., 2007). The approach has allowed imaging of the distribution of glycogen in tissue, and monitoring its metabolism non-invasively in magnetic resonance imaging experiments. Similarly the present study showed that the enzymic breakdown of starch to glucose could also be monitored via changes in the *z*-spectra of samples. Exploring the possibilities of CEST paves the way for the implementation of the technique in circumstances when non-exchangeable proton signals cannot be readily measured using ^{1}H NMR, while exchangeable protons can be detected.

4. Conclusions

Chemical exchange saturation transfer has been successfully implemented to explore and monitor the enzymic degradation of macromolecular starch granules. Applying understanding of the features observed in the CEST *z*-spectrum of glucose, both the kinetics of mutarotation between anomers of glucose and the kinetics of glucose release during the hydrolysis by glucoamylase of cooked starch was successfully monitored. Using CEST to monitor reaction kinetics holds much promise in biochemical systems where relevant signals from non-exchangeable protons are not able to be accurately monitored by classical ^{1}H NMR methods. Alternately CEST can be used to monitor the change in the nature of protons in relatively fast exchange with aqueous solvent to observe the kinetics of biochemical systems.

Acknowledgment

P.W.K. gratefully acknowledges the support of Australian Research Council Grant DP0877789.

References

Ao, Z., Simsek, S., Zhang, G., Venkatachalam, M., Reuhs, B. L., & Hamaker, B. R. (2007). Starch with a slow digestion property produced by altering its chain length, branch density, and crystalline structure. *Journal of Agricultural and Food Chemistry*, *55*, 4540–4547.

Barclay, A. W, Petocz, P., McMillan-Price, J., Flood, V. M., Prvan, T., Mitchell, P., et al. (2008). Glycemic index, glycemic load, and chronic disease risk – A meta-analysis of observational studies. *American Journal of Clinical Nutrition*, *87*, 627–637.

Brand-Miller, J. C., Holt, S. H. A., Pawlak, D. B., & McMillan, J. (2002). Glycemic index and obesity. *American Journal of Clinical Nutrition*, *76*, 281S–285S.

Brindle, K. M., Brown, F. F., Campbell, I. D., Grathwohl, C., & Kuchel, P. W. (1979). Application of spin-echo nuclear magnetic resonance to whole-cell systems. Membrane transport. *Biochemical Journal*, *180*, 37–44.

Cho, S. I., Bellon, V., Eads, T. M., Stroshine, R. L., & Krutz, G. W. (1991). Sugar content measurement in fruit tissue using water peak suppression in high resolution proton magnetic resonance. *Journal of Food Science*, *56*, 1091–1094.

Chung, H.-J., Yoo, B., & Lim, S.-T. (2005). Effects of physical aging on thermal and mechanical properties of glassy normal corn starch. *Starch/Starke*, *57*, 354–362.

Chung, H.-J., Lim, H. S., & Lim, S.-T. (2006). Effect of partial gelatinization and retrogradation on the enzymatic digestion of waxy rice starch. *Journal of Cereal Science*, *43*, 353–359.

DeVries, J. W. (2007). Glycemic index: The analytical perspective. *Cereal Foods World*, *52*, 45–49.

Dona, A., Yuen, C.-W. W., Peate, J., Gilbert, R. G., Castignolles, P., & Gaborieau, M. (2007). A new NMR method for directly monitoring and quantifying the dissolution kinetics of starch in DMSO. *Carbohydrate Research*, *342*, 2604– 2610.

Dona, A. C., Pages, G., Gilbert, R. G., Gaborieau, M., & Kuchel, P. W. (2009). Kinetics of *in vitro* digestion of starches monitored by time-resolved ^{1}H nuclear magnetic resonance. *Biomacromolecules*, *10*, 638–644.

Fabri, D., Williams, M. A. K., & Halstead, T. K. (2005). Water T_2 relaxation in sugar solutions. *Carbohydrate Research*, *340*, 889–905.

Forsen, S., & Hoffman, R. A. (1963). Study of moderately rapid chemical exchange reactions by means of nuclear magnetic double resonance. *Journal of Chemical Physics*, *39*, 2892–2901.

French, D., & Knapp, D. W. (1950). The maltase of *Clostridium acetobutylicum*. Its specificity range and mode of action. *Journal of Biological Chemistry*, *187*, 463–471.

Garsetti, M., Vinoy, S., Lang, V., Holt, S., Loyer, S., & Brand-Miller, J. C. (2005). The glycemic and insulinemic index of plain sweet biscuits: Relationships to *in vitro* starch digestibility. *Journal of American Nutrition*, *24*, 441–447.

Goffeney, N., Bulte, J. W. M., Duyn, J., Bryant, L. H., Jr., & van Zijl, P. C. M. (2001). Sensitive NMR detection of cationic-polymer-based gene delivery systems using saturation transfer via proton exchange. *Journal of the American Chemical Society*, *123*, 8628–8629.

Goni, I., Garcia-Alonso, A., & Saura-Calixto, F. (1997). A starch hydrolysis procedure to estimate glycemic index. *Nutrition Research (New York)*, *17*, 427–437.

Guivel-Scharen, V., Sinnwell, T., Wolff, S. D., & Balaban, R. S. (1998). Detection of proton chemical exchange between metabolites and water in biological tissues. *Journal of Magnetic Resonance*, *133*, 36–45.

Jenkins, D. J. A., Kendall, C. W. C., Augustin, L. S. A., Franceschi, S., Hamidi, M., Marchie, A., et al. (2002). Glycemic index: Overview of implications in health and disease. *American Journal of Clinical Nutrition*, *76*, 266S–273S.

Kendrew, J. C., & Moelwyn-Hughes, E. A. (1940). Kinetics of mutarotation in solution. *Royal Society (London) A*, *176*, 352–367.

Kerr, R. W., Cleveland, F. C., & Katzbeck, W. J. (1951). The action of amyloglucosidase on amylose and amylopectin. *Journal of the American Chemical Society*, *73*, 3916–3921.

Kim, M., Gillen, J., Landman Bennett, A., Zhou, J., & van Zijl, C. M. P. (2009). Water saturation shift referencing (WASSR) for chemical exchange saturation transfer (CEST) experiments. *Magnetic Resonance Medicine*, *61*, 1441– 1450.

Kruger, J. E., & Marchylo, B. A. (1985). A comparison of the catalysis of starch components by isoenzymes from the two major groups of germinated wheat α-amylase. *Cereal Chemistry*, *62*, 11–18.

Kuchel, P. W., Bulliman, B. T., Chapman, B. E., & Kirk, K. (1987). The use of transmembrane differences in saturation transfer for measuring fast membrane transport; application to carbon-13-labeled biocarbonate exchange across the human erythrocyte. *Journal of Magnetic Resonance*, *74*, 1–11.

Kuchel, P. W., Bulliman, B. T., & Chapman, B. E. (1988). Mutarotase equilibrium exchange kinetics studied by ^{13}C NMR. *Biophysical Chemistry*, *32*, 89– 95.

Labotka, R. J., Lundberg, P., & Kuchel, P. W. (1995). Ammonia permeability of erythrocyte membrane studied by ^{14}N and ^{15}N saturation transfer NMR spectroscopy. *American Journal of Physiology*, *268*, 686–699.

Livesey, G., Taylor, R., Hulshof, T., & Howlett, J. (2008). Glycemic response and health – A systematic review and meta-analysis: Relations between dietary glycemic properties and health outcomes. *American Journal Clinical Nutrition*, *87*, 258S–268S.

McConnell, H. M., & Thompson, D. D. (1959). Molecular transfer of nonequilibrium nuclear spin magnetization. *Journal of Chemical Physics*, *30*, 85– 88.

McMahon, M. T., Gilad, A. A., Zhou, J. Y., Sun, P. Z., Bulte, J. W. M., & van Zijl, P. C. M. (2006). Quantifying exchange rates in chemical exchange saturation transfer agents using the saturation time and saturation power dependencies of the magnetization transfer effect on the magnetic resonance imaging signal (QUEST and QUESP): pH calibration for poly-L-lysine and a starburst dendrimer. *Magnetic Resonance in Medicine*, *55*, 836–847.

Mukerjea, R., Slocum, G., Mukerjea, R., & Robyt, J. F. (2006). Significant differences in the activities of α-amylases in the absence and presence of polyethylene glycol assayed on eight starches solubilized by two methods. *Carbohydrate Research*, *341*, 2049–2054.

Mulquiney, P. J., Bubb, W. A., & Kuchel, P. W. (1999). Model of 2,3-bisphosphoglycerate metabolism in the human erythrocyte based on detailed enzyme kinetic equations: *In vivo* kinetic characterization of 2,3-bisphosphoglycerate synthase/phosphatase using ^{13}C and ^{31}P NMR. *The Biochemical Journal*, *342*, 567–580.

Okuda, M., Aramaki, I., Koseki, T., Satoh, H., & Hashizume, K. (2005). Structural characteristics, properties, and *in vitro* digestibility of rice. *Cereal Chemistry*, *82*, 361–368.

Szekely, D., Chapman, B. E., Bubb, W. A., & Kuchel, P. W. (2006). Rapid exchange of fluoroethylamine via the Rhesus complex in human erythrocytes: ^{19}F NMR magnetization transfer analysis showing competition by ammonia and ammonia analogues. *Biochemistry*, *45*, 9354–9361.

Thompson, D. B. (2000). On the non-random nature of amylopectin branching. *Carbohydrate Polymers*, *43*, 223–239.

Thornley, S., McRobbie, H., Eyles, H., Walker, N., & Simmons, G. (2008). The obesity epidemic: Is glycemic index the key to unlocking a hidden addiction? *Medical Hypotheses*, *71*, 709–714.

van Zijl, P. C. M., Jones, C. K., Ren, J., Malloy, C. R., & Sherry, A. D. (2007). MRI detection of glycogen *in vivo* by using chemical exchange saturation transfer imaging

(glycoCEST). *Proceedings of the National Academy of Sciences of the United States of America*, *104*, 4359–4364.

Wolever, T. M. S., Mehling, C., Chiasson, J. L., Josse, R. G., Leiter, L. A., Maheux, P., et al. (2008). Low glycaemic index diet and disposition index in type 2 diabetes (the Canadian trial of Carbohydrates in Diabetes): A randomised controlled trial. *Diabetologia*, *51*, 1607–1615.

Woods, M., Woessner, D. E., Zhao, P. Y., Pasha, A., Yang, M. Y., Huang, C. H., et al. (2006). Europium(III) macrocyclic complexes with alcohol pendant groups as chemical exchange saturation transfer agents. *Journal of the American Chemical Society*, *128*, 10155–10162.

Zhang, S., Merritt, M., Woessner, D. E., Lenkinski, R. E., & Sherry, A. D. (2003). PARACEST agents: Modulating MRI contrast via water proton exchange. *Accounts of Chemical Research*, *36*, 783–790.

Zhou, J., & van Zijl, P. C. M. (2006). Chemical exchange saturation transfer imaging and spectroscopy. *Progress in Nuclear Magnetic Resonance Spectroscopy*, *48*, 109–136.

Zhou, J., Wilson, D. A., Sun, P. Z., Klaus, J. A., & van Zijl, P. C. M. (2004). Quantitative description of proton exchange processes between water and endogenous and exogenous agents for WEX, CEST, and APT experiments. *Magnetic Resonance in Medicine*, *51*, 945–952.